Leukocyte-Platelet-Rich Plasma (L-PRP) Induces an Abnormal Histophenotype in Craniofacial Bone Repair Associated with Changes in the Immunopositivity of the Hematopoietic Clusters of Differentiation, Osteoproteins, and TGF-β1

Allan Fernando Giovanini, PhD;* João Ricardo Almeida Grossi, Msc;† Carla Castiglia Gonzaga, PhD;* João Cesar Zielak, PhD;* Isabella Göhringer, DDS;† Juliana de Souza Vieira, DDS;† Juliane Kuczera, DDS;‡ Marco Antonio de Oliveira Filho, PhD;§ Tatiana Miranda Deliberador, PhD*

ABSTRACT

Background: Leukocyte-platelet-rich plasma (L-PRP) is considered an important source of growth factors, especially Transforming growth factor β 1 (TGF-β1), which modulates the proliferation and regulation of mesenchymal cells, and also exerts an influence on the hematopoiesis, osteogenesis, and adipogenesis in bone microenvironment. Thus, the aim of this study was to evaluate the effect of L-PRP on the calvarial bone repair and compare its results on the presence of TGF-β1, CD34, CD45, bone morphogenetic protein 2 (BMP2), BMPR1B, and Runx2 proteins detected by immunohistochemistry.

Material and Methods: Four bone defects were created on the calvaria of 23 rabbits. The defects were treated with autograft, L-PRP alone, and L-PRP mixed with autograft. The animals were euthanized at 2, 4, and 6 weeks post-surgery.

Results: Unlike autograft and sham groups, the defects treated with L-PRP demonstrated significant positivity to TGF-β1, while the BMP2 was scarce. These results coincided with the lower bone matrix deposited and larger medullary area, which were composed of fibrosis, when treated with only L-PRP, or intense adiposity on defects filled with L-PRP mixed with autograft. The fibrosis that occurred was associated with a minor percentage of osteoproteins, intense presence of $CD34^{+}CD45^{-}$ cells, and significant expression of TGF-β1 in all time periods analyzed. The adiposity occurred from the major presence of osteoprogenitor $BMPR1B^{+}$ $Runx2^{+}$ cells simultaneously to $BMP2^{-}TGF\text{-}\beta1^{+}$ and $CD34^{+}CD45^{+/-}$ expressions predominantly on the earlier period.

Conclusion: From this study, it can be concluded that the L-PRP used alone or mixed to autograft hindered the osteoneogenesis due to suppression of immunoexpression of BMP2, while the immunopositivity of TGF-β1 was intense. When used alone, the L-PRP induced a fibrotic condition associated with TGF-β1 presence and lack of osteoproteins, but when L-PRP was mixed to autograft, it induced the presence of the osteolineage cells ($BMPR1B^{+}Runx2^{+}$), but also inhibited the terminal osteoblastic maturation associated with the lack of BMP2 and the presence of $TGF\text{-}\beta1^{+}$, a fact that contributed to cellular transdifferentiation into fat cells.

KEY WORDS: BMP-2, bone regeneration, CD34, CD45, Runx2, platelet-rich plasma

INTRODUCTION

Platelet-rich plasma (PRP) consists of autogenous blood-derived fractions composed of high concentrations of platelets[1–3] and is considered to be an important source of growth factors when activated by either agonist or collagen interactions at the injury sites.[4,5] These growth factors are supposed to have a stimulating effect on several types of cells involved in the initial stages of bone wound healing, regulating both its

*Professors of Masters Program in Clinical Dentistry, Positivo University, Curitiba, Brazil; †graduate students of Masters Program in Clinical Dentistry, Positivo University, Curitiba, Brazil; ‡undergraduate student, School of Dentistry, Positivo University, Curitiba, Brazil; §Head and Neck Surgery Service, Evangelic Hospital, Curitiba, Brazil

Reprint requests: Dr. Allan Fernando Giovanini, Positivo University, Rua Pedro Viriato Parigot de Souza #5300, Curitiba – Paraná 81280-330, Brazil; e-mail: afgiovanini@gmail.com

DOI 10.1111/j.1708-8208.2012.00478.x

morphogenesis and differentiation, while also contributing to enhanced bone formation.[6,7] Despite this attractive rationale, some clinical results and analysis of the animal research have not revealed consistent and reliable results, generating confusion regarding the real beneficial effect of PRP in the bone repair.[8–10]

Actually, the difference of opinion about the effect of PRP on the osteoneogenesis has been speculated upon, especially in the variations in the PRP confections. In recent review, Arnoczky and colleagues[11] indicate that PRP preparations may include white blood cells (leukocytes) in their final product. The presence of the white blood cells is known to play a key role in the initial phases of inflammation and there is significant doubt about the real potential benefits of the white blood cells in PRP preparations, a fact that may contribute to the variation of results found in the literature when PRP is used. In fact, a clear definition of what qualifies the PRP as leukocyte poor or leukocyte rich does not yet exist. Commonly, when most authors refer to leukocyte-poor PRP, they describe a product that has had leukocytes intentionally removed from the collected blood solution,[12] as performed by Marx and colleagues.[13] However, most studies do not mention this leukocyte removal during the PRP production. In these cases, the PRP has been considered only as a fraction of the buffy coat (rich in platelet and leukocytes) associated with small amounts of plasma obtained during the centrifugation process.[11,12] Thus, studies using leukocytes-rich PRP (L-PRP) remain a likely alternative to study of the bone repair. This hypothesis has been considered since the fraction that contains white blood cells may also contain considerable quantities of the CD34+ stem cells, which is a progenitor cell derived from medullary lineage. A recent study reported by Giovanini and colleagues[14] revealed inhibited bone healing in a PRP-treated rabbit calvarial defect model despite elevated levels of CD34+ cells.

Apart from this, the presence of the CD34+ cells is also expected when the L-PRP is used, since platelets induce the chemotaxy of the CD34 stem cells. In this work, we hypothesized that the L-PRP could alter the biology of the calvaria bone repair, changing the biology of the CD34+ cells differentiation.

This hypothesis is plausible since CD34 originates in the hematopoietic cells, adipose, and bone. Yet, the development for each tissue that compounds the bone/medullary tissue is a complex process, given that the bone marrow and bone are anatomically contiguous tissues.[15–17] They share an ordinary growth factor (Transforming growth factor [TGF]-β1) in their development or inhibition.[18,19] In addition, the lineage of the CD34 cell may be functionally different, and be defined as multipotent hematopoietic stem cells when associated with a lack of CD45 ($CD34^+CD45^-$ lineage) or long-term self-renewal cells, which have the ability to give themselves only, when $CD34^+$ cells are co-expressed with a CD45 immunophenotype ($CD34^+CD45^+$ lineage).[20]

The hematopoiesis is associated with primitive stem cell proliferation and differentiation. It involves a sufficient and constant production of bone marrow maturing cells, which includes both erythroid and myeloid lineages.[21,22] All leukocytes and nucleated hematopoietic cells are characterized by unique cell surface expression CD45, which has been shown to regulate and express in all stages of both myeloid and lymphoid maturation.[23–25]

Other proteins are also commonly expressed and they have an important impact on cellular differentiation from CD34 stem cells. For example, the activation of some of the proteins and transcription factors and, consequently, the repression of others is essential for the commitment of cells to a specific differentiation lineage. The presence of these proteins may indicate the pattern characteristic for the particular type of cells, especially in bone development, while the adipose differentiation pathways are inhibited.[16,26] In this way, the bone morphogenetic protein 2 (BMP2) is a crucial participant in postnatal skeletal homeostasis, and the signal provided by this protein is required for the inherent reparative capacity of bone.[27–29] In calvarias, the biological activities of BMP2 are mediated through binding to active receptors subunits (BMPRs), especially BMPR1B.[30] When BMP2 and BMPR1B interact, it stimulates the Runt-related transcription factor-2 (Runx2), a transcription factor necessary for early differentiation of osteoblasts.[27,31–33]

On the other hand, BMPR1B is a TGF receptor family of serine/threonine kinases that also may interact with TGF-β1 cytokine that, similarly to BMP2, also induces the Runx2 expression. Nevertheless, some studies have shown that the osteoneogenesis may be inhibited when either BMP2 – BMPR1B – Runx2 signal failure or the BMPR1B is trunked or overexpressed, favoring adipose development,[34] while other studies indicate that the presence of BMPR1B and Runx2 induced by highest levels of TGF-β1 not only increases bone deposition but also occurs more quickly.[3,13]

Thus, based on principle that TGF-β1 influences in the hematopoiesis, osteogenesis, and adipogenesis,[19] the aim of this study was to evaluate the effect of L-PRP on the calvaria bone repair and compare its results on the presence of TGF-β1, CD34, CD45, BMP2, BMPR1B, and Runx2 proteins detected by immunohistochemistry.

MATERIALS AND METHODS

Twenty-three New Zealand female rabbits, ranging in age from 350 to 370 days and weighing 2.75 to 4.60 kg, and with no previous disease, were used following a protocol approved by the Institutional Animal Care and Use Committee of Positivo University (Curitiba, PR, Brazil). The rabbits were kept in a room with a controlled temperature (approximately 22°C) and maintained under a 12-hour light/dark cycle.

PRP Fabrication and Its Quantification

A 15-ml sample of autologous blood was collected from each animal through cannulation of the ear vein into a syringe containing 1.48 ml of 10% sodium citrate. The blood samples were centrifuged at $200 \times g$ for 20 minutes at room temperature to separate the plasma containing the platelets from the red cells (Beckman J-6 M Induction Drive Centrifuge; Beckman Instruments Inc., Palo Alto, CA, USA). The plasma fraction was collected from the top of the supernatant. The remaining fractions were centrifuged once more at room temperature for 10 minutes at $400 \times g$ to separate the platelets. The platelet-poor plasma was removed from the upper level of the supernatant, leaving the PRP and buffy coat. Both the PRP (1.0 ml) and the buffy coat were resuspended and activated with a mixture of 10% calcium chloride (0.05 ml/ml of PRP). They were then added to the previously prepared L-PRP and mixed for approximately 1 minute until they formed a gel.

The platelets and leukocytes on the L-PRP were measured after centrifugation using a Coulter STKS hematology-counting machine (Beckman-Coulter, Chicago, IL, USA). An average of $2.414 \times 10^6 \pm 1.547 \times 10^6$ platelets/μl was achieved. In addition, the morphological integrity and concentration of more than five times enrichment of L-PRP were confirmed, whereas initial values accounted for approximately $3.014 \times 10^5 \pm 1.056 \times 10^5$ platelets/μl. Simultaneously, an average of $4.383 \times 10^4 \pm 0.817 \times 10^4$ leukocytes/μl were measured in the L-PRP, while the initial blood values account were $9.381 \times 10^3 \pm 0.108 \times 10^3$ leukocytes/μl.

Surgical Procedure

The rabbits were anesthetized by an intramuscular injection of xylazine (5 mg/kg) and ketamine (70 mg/kg). The surgical region was shaved and aseptically prepared, and sterile barriers were created to limit the surgical area. A 5-cm midline dermo-periosteal incision was made to expose the calvarial surface. Four circular artificial defects of 8 mm in diameter × 2 mm in depth were created with a trephine (Biomedic Research Instruments Inc., Silver Springs, MD, USA) under abundant saline solution irrigation.

Bone fragments removed from the calvarias defects were particulated and used for autograft. One defect was filled with 0.01 ml of autograft (group I), another was filled with 0.01 ml of autograft associated with 100 μl of L-PRP (group II), and a third was filled with 100 μl of L-PRP alone (group III). The control animals (sham) underwent the same surgical procedures without the use of any grafting material (group IV). Soft tissues were repositioned and sutured to achieve primary closure (4.0 silk, Ethicon, Sao Paulo, SP, Brazil). Each animal received a prophylactic intramuscular injection of 24,000 IU of penicillin G benzathine.

Euthanasia Procedure and Tissue Processing

The animals were euthanized by brief exposure in a CO_2 chamber until they ceased moving after 2 weeks (eight animals), 4 weeks (eight animals), and 6 weeks (seven animals) post-surgery. The skull caps of the animals were removed in blocks, using an inverted cone bur. Necropsied calvaria specimens were fixed in 10% buffered formalin for 48 hours and decalcified in 20% formic acid and sodium citrate for 7 days. The specimens were washed with tap water, dehydrated, diafanized, and embedded in paraffin. Serial sections of 3-μm perpendiculars to the midsagittal suture were cut from the center of each defect, using a microtome (RM2155, Leica Microsystems GmbH, Nussloch, Germany) and stained with Masson's trichrome to permit histomorphological and histomorphometric evaluation.

Immunohistochemistry Processing

Three-micrometer thicknesses of each specimen were deparaffinized and subjected to antigen retrieval in 1% trypsin solution (pH 6.8) for 60 minutes at 37°C for the anti-BMP2, BMPR1B, Runx2, and TGF-β1 antibodies and in 10 mM citrate solution (pH 6.0) for 45 minutes in a double-boiler at 95°C for the anti-CD34 and CD45

antibodies. The slides containing the histological specimens were immersed in 3% hydrogen peroxide for 30 minutes to eliminate endogenous peroxidase activity, followed by incubation with 1% phosphate-buffered saline (pH 7.4). The sections were incubated with the primary antibody anti-TGF-β1 (200 μg/ml, Santa Cruz Biotechnology Inc., sc 146, CA, USA) with a dilution factor of 1:200, anti-BMP2 (0.5 mg/ml, Abcam, Cambridge, UK, ab 6285) with a dilution factor of 1:150, anti-BMPR1B (200 μg/ml, Santa Cruz Biotechnology Inc., sc 25455) with a dilution factor of 1:300, anti-Runx2 (100 μg at 1 mg/ml, Abcam, ab 23981, Cambridge, UK) anti-CD34 (0.9 mg/ml, Clone QBEnd 10 – DAKO, Glostrup, Denmark) with a dilution factor of 1:200, and CD45 (1.0 mg/ml, Clone 2D1 – DAKO, Glostrup, Denmark) diluted 1:250. The labeled streptavidin biotin antibody-binding detection system (Universal HRP immunostaining kit – Diagnostic Byosystem Universal HRP Immunostaining Kit, Diagnostic Byosystem, Foster City, CA, USA) was employed to detect the primary antibodies. The immune reaction was observed with the diaminobenzidine tetrachloride chromogen solution (Universal HRP Immunostaining Kit, Diagnostic Byosystem, Foster City, CA, USA), which produced a brown precipitate at the antigen site. The specimens were counterstained with Mayer's hematoxylin. A negative control was performed for all samples, using rabbit polyclonal isotype IgG (2 μg/ml, Abcam, ab 27472, Cambridge, UK) for 10 minutes at room temperature as a primary antibody. For each specimen, three slides were utilized for incubation with each antibody.

Image Analysis

The images of both the histological and immunohistochemistry sections were captured by a digital camera (SDC-310, Samsung, Kyungki-Do, South Korea) coupled at a light microscope (Zeiss, Germany) with an original magnification of ×200. Each digital image was gathered and preserved with 600 dpi resolution, producing a virtual frame of 117 × 80 cm. Because it was not possible to capture the entire defect in one image at the magnification level used, a composite digital image of the whole defect was then constructed by combining two smaller images based on histomorphological reference structures, especially the deposited bone trabeculae and blood vessels.

All histomorphometric and immunohistochemical measurements were completed using the software ImageJ (National Institute of Health, Bethesda, MD, USA). An image of 1-mm slide was used to calibrate all measurements. The histomorphometric data were counted manually and expressed as areas (mm^2). The perimeters of the deposited histological bone matrix and each bone marrow areas were carefully traced, all areas were computed, and their values were transformed into percentages (each area measured/total area). At the same time, the percentage of positive CD34 and CD45 cells/mm^2 was manually counted and tagged, while the percentage of positivity to BMP2, BMPR1B, Runx2, and TGF-β1 was accounted by automation, following the protocol established by Di Cataldo and colleagues.[35] This automated counting allowed counting only the percentage of protein present in the whole defect; it is not possible to distinguish their genuine immunostaining in cells or bone matrix.

Statistical Analysis

Each parameter was evaluated within the monitoring period. An analysis of variance was used to determine if there were significant differences among groups, followed by Student–Newman–Keul's nonparametric test. A p value of less than .05 was considered to be statistically significant.

RESULTS

Light Microscopic Analysis

The quantitative data of the histomorphometric analysis is demonstrated in Figure 1. A brief description of the microscopic characteristics found among groups is provided as follows and demonstrated in Figure 2.

Group I (Autograft). On the 2nd week post-operative, both bone fragments exhibiting basophilic reversal lines and new bone formation from the autograft bone were present. In addition, a few granulation tissues were observed. Some leukocytes and myeloid cells, as well as adipocytes, were present in the medullary area formed. On the 4th week post-surgery, a new compact haversian bone formed was identified. Furthermore, areas composed of scarce fibrous tissue were present, and they were restricted in both well-formed bone marrow and periosteum. From the 4th to the 6th post-surgery week, insignificant changes were noted in both the bone deposition and the medullary area.

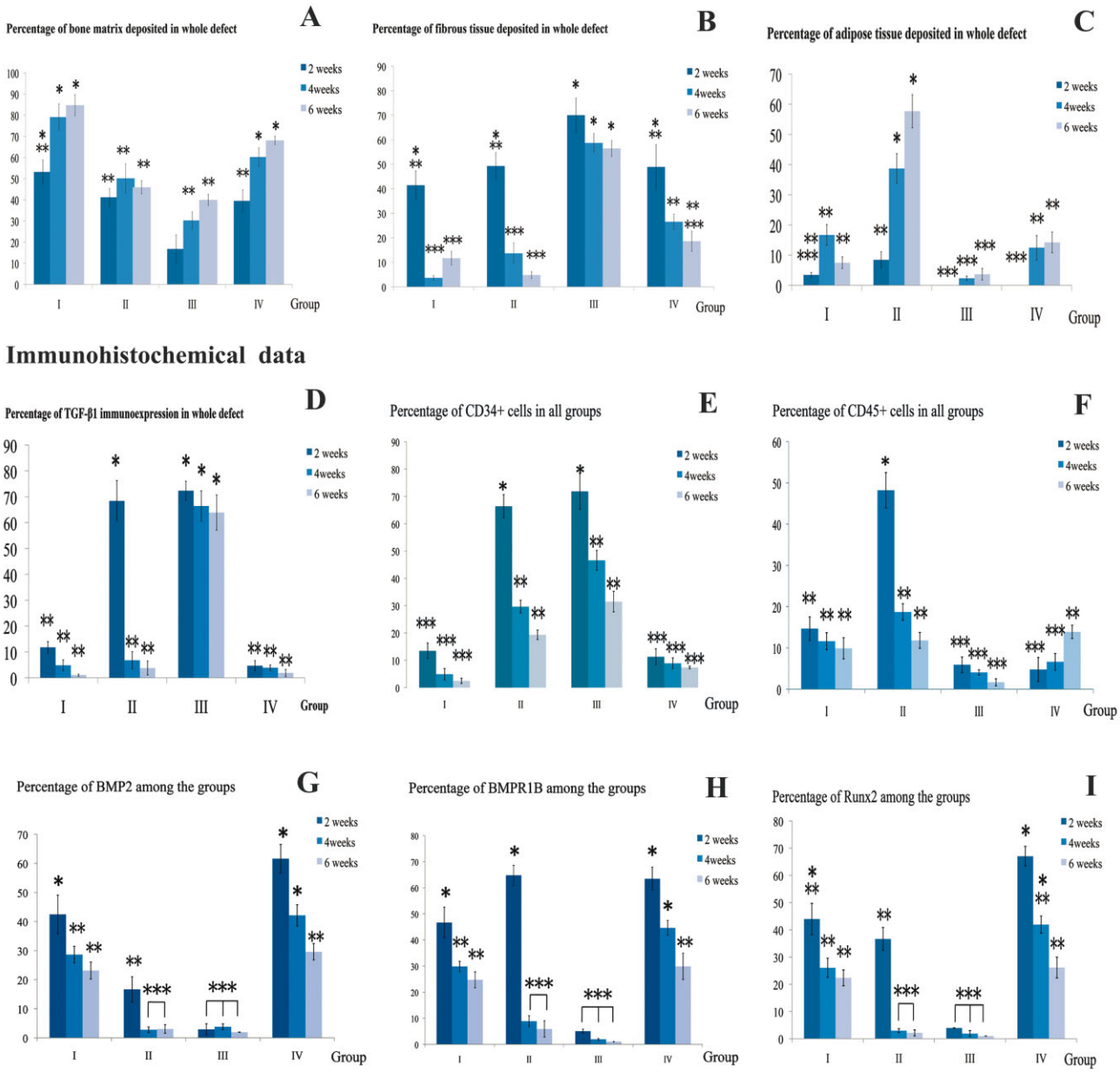

Figure 1 Graphical comparison among the groups analyzed. Graphics A, B, and C give the mean and standard deviation of the histomorphometric data in percentage. D, E, and F reveal the mean and standard deviation of the immunohistochemistry data in percentage. Bars followed by the same superscript are statistically similar, $p > .05$, while Roman numerals correspond each group (I–IV).

Group II (L-PRP Mixed with Autograft). On the 2nd week post-surgery, inserted bone fragments were detected surrounded by rich mesenchymal cellular tissue. From the 2nd to the 4th post-surgery week, the amount of deposited bone matrix increased slightly, and a substantial quantity of fat cells was found. Interestingly, on the 6th week post-surgery, the amount of both bone matrix area and adipose tissue was similar to that found on the 4th week post-surgery.

Group III (L-PRP). Histological analysis conducted after the 2nd post-surgery week revealed intensive mesenchymal tissue. Discrete immature bone tissue in the adjacent host bone area located peripherally to the defect completed the histological frame. On the 4th post-surgery week, the microscopic analysis revealed an increase in immature bone tissue located peripherally to the surgical bed. However, a larger quantity of fibrous tissue was found on the 4th and 6th week post-surgery.

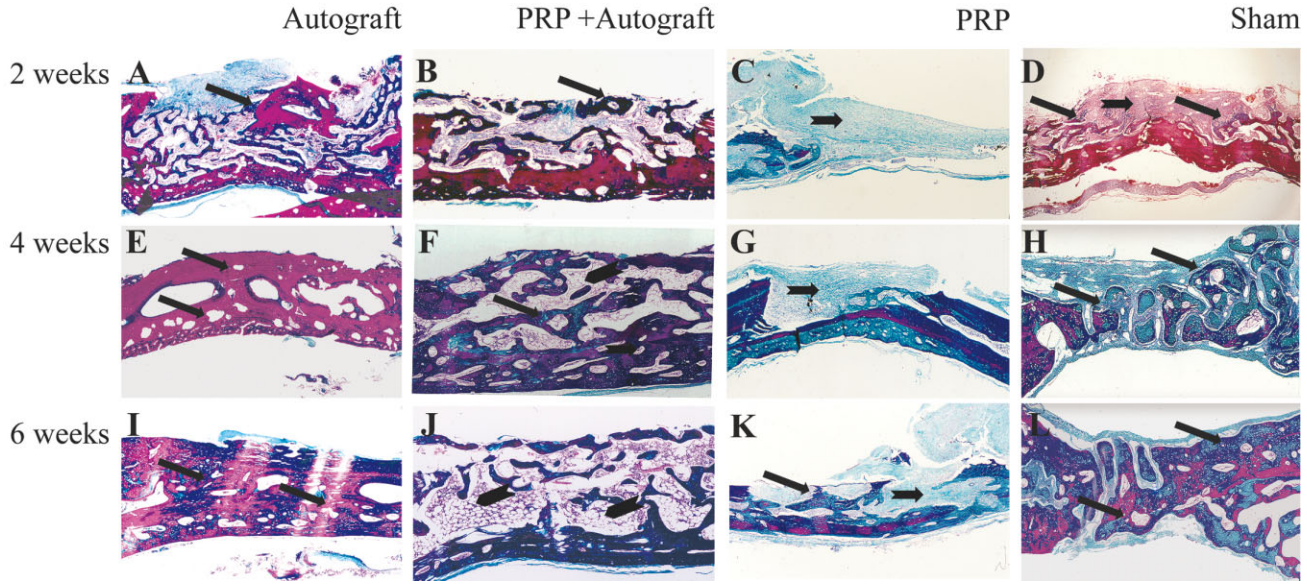

Figure 2 Histological features of all studied groups in the all time period. Micrographs A, E, and I reveal the histological illustration of group I (autograft) and demonstrate robust new haversian bone formation (*arrows*), respectively, on 2nd, 4th, and 6th week post-operative. The micrographs B, F, and J show the repair in group II (PRP mixed to autograft), respectively, on the 2nd, 4th, and 6th week post-operative. Identify the bone grafted (*arrows*) and the significant adiposity development (chevron) similarly to osteoporotic bone. The histological features of the group that received only PRP (group III) are present on the micrographs C, G, and K, respectively, on the 2nd, 4th, and 6th week. This group reveals intensive fibrosis in all period analyzed (Notched arrow) with lower bone matrix deposition (*arrows*). D, H, and L micrographs demonstrate the bone repair in the sham group (control) on the 2nd, 4th, and 6th week post-operative. This group demonstrated a significant haversian bone matrix, especially on the 4th and 6th week post-surgery (All micrograph stained with Masson's trichrome, at original magnification ×40).

Group IV (Control – Sham). On the 2nd week post-surgery, the microscopic analysis revealed areas of granulation tissue composed of collagen and mesenchymal cells in the larger part of the defect. Furthermore, there was evidence of newly formed immature bone that mimicked intramembranous ossification. Four weeks after surgery, granulation tissue was detected around a substantial quantity of both mature and immature haversian bone tissue. From the 4th to the 6th week post-operative, significant haversian bone was detected.

Immunohistochemical Results

A percentage of the quantitative data of the immunohistochemistry is given in Figure 1 ($p < .05$). In summary, the results can be described as follows.

TGF-β1. On the 2nd week post-surgery, all groups analyzed demonstrated positivity to TGF-β1, as seen in Figure 3. In the groups filled with L-PRP (groups II and III), the immunopositivity was intense and the percentage of positivity of TGF-β1 was considerably higher than in the L-PRP-free groups (Figure 1). On the 4th and 6th post-operative weeks, the pattern of TGF-β1 expression in group III (only L-PRP) remained similar to the 2nd week post-surgery, while the percentage of TGF-β1 decreased significantly in the both L-PRP-free and L-PRP mixed with autograft groups between the 4th and the 6th post-surgery weeks.

BMP2. On the 2nd week post-surgery, all groups demonstrated positivity to BMP2 (Figure 4). Furthermore, the percentage of positivity to BMP2 was markedly higher in the L-PRP-free group. The highest values of this protein were observed in the control group and occupied whole mesenchymal tissue, while in group I (autograft), the protein was concentrated in the adjacencies of the engraft bone. In contrast, in groups II (L-PRP associated with autograft) and III (only L-PRP), few cells and matrix exhibited positivity to BMP2 and they were restricted to adjacencies on the bone grafted or concentrated peripherally to the host bone. They were scarce around the artificial defect and among the grafted bone fragments. A similar pattern was observed either on the 4th or 6th (Figure 5) week post-surgery; therefore, their values decreased as soon as fatty cells, hematopoietic cells, or when the bone matrix appeared.

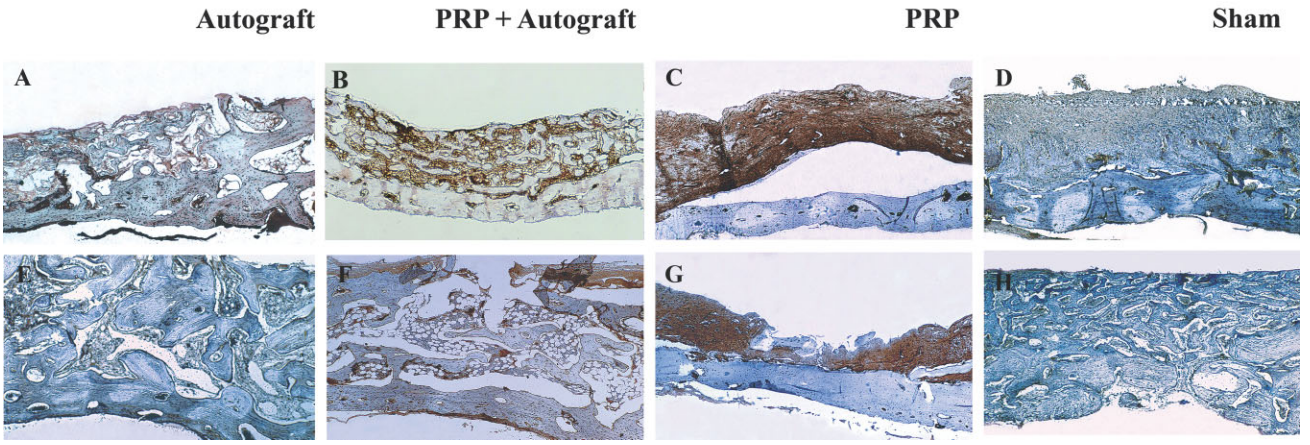

Figure 3 The TGF-β1 analysis. The immunoexpression (brownish colored) among the groups analyzed are demonstrated in the micrographs A to H. Micrographs A to D reveal respectively the presence of the TGF-β1 in the autograft, p-PRP mixed with autograft and alone and sham groups on 2nd week post-surgery. The immunohistochemistry analysis demonstrates higher presence to the cytokine in the p-PRP groups (B and C), while in the control and autograft groups, the presence of TGF-β1 is scarce. The micrographs E, F, and H show the decreased of the immunoexpression to TGF-β1 in the autograft, p-PRP mixed with autograft and sham group on the 4th week post-surgery, while the expression to the cytokine is significant on the group p-PRP alone on the 6th week post-operative (G) (magnification ×40, except E and F, ×100).

BMPR1B. All groups exhibited positivity to BMPR1B in the earlier period, as seen in Figure 4. On the 2nd post-surgery week, the expressions were evident in the L-PRP-free groups, especially in the cellular matrix that surrounded the bone fragment grafted (group I) or spread across the artificial defect (group IV). However, the groups that received L-PRP treatment demonstrated different results when associated with autograft (group II) and L-PRP alone (group III). The group that received only L-PRP (group III) showed scarce positivity to BMPR1B among the mesenchymal tissue. On the other hand, a higher quantity of cells that exhibited positivity

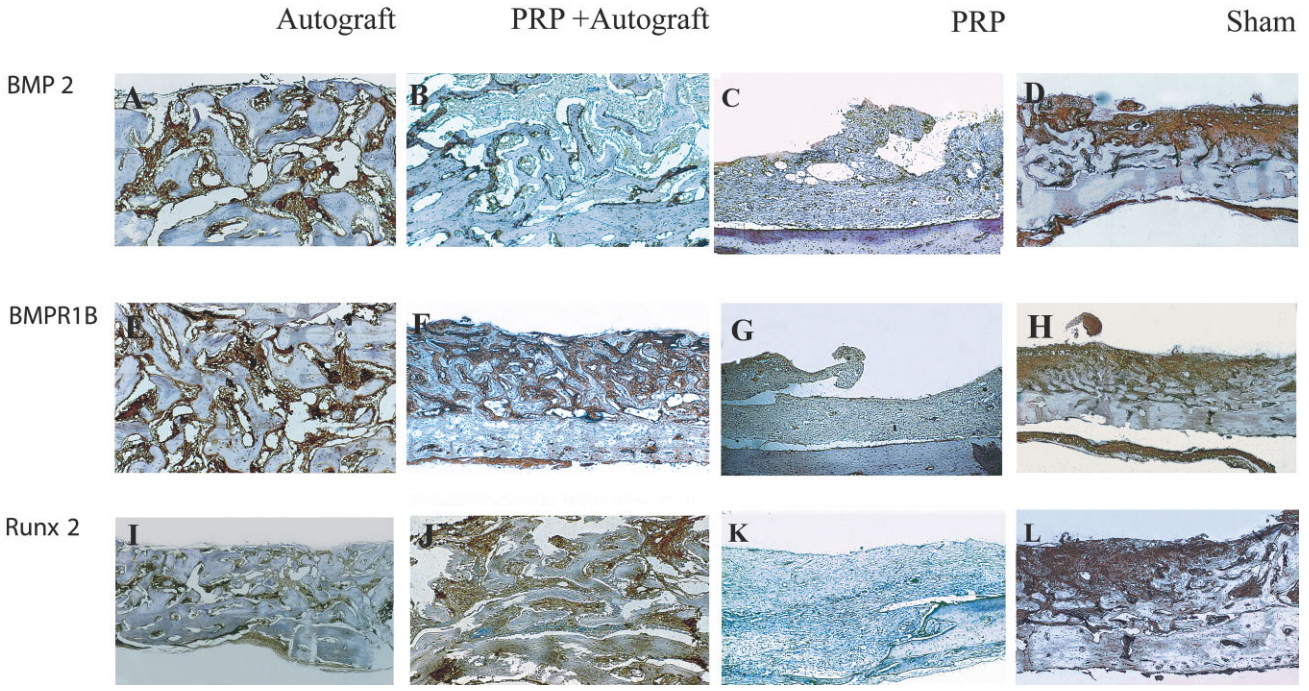

Figure 4 The osteoproteins analysis on 2nd week post-surgery. A to D show the quantities of the presence of the BMP2 in whole defect, while E to H and I to L reveal respectively the characteristics of the BMPR1B and Runx2 immunoexpression in each group (magnification ×40, except A, B and E, ×100).

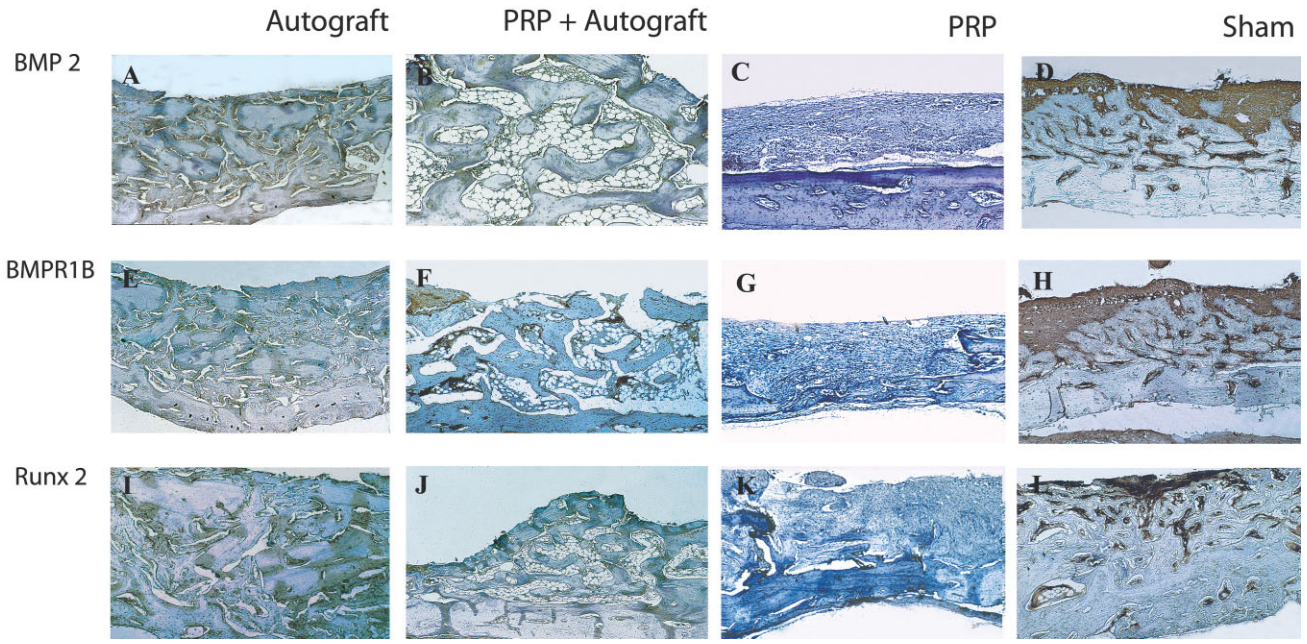

Figure 5 The osteoproteins analysis on 6th week post-surgery. A to D show the quantities of the presence of the BMP2 in whole defect, while E to H and I to L reveal respectively the characteristics of the BMPR1B and Runx2 immunoexpression in each group (magnification ×40, except B and I, ×100).

to BMPR1B were found in group II, and they occupied the entire defect around the grafted bone fragment. On the 4th and 6th (Figure 5) week post-surgery, the quantity of BMPR1B+ cells decreased significantly, while a fibrotic (group III) or adipose tissues (group II) were formed in the L-PRP groups. Yet, groups I and II demonstrated positivity to BMPR1B concentrated to bone matrix deposited.

Runx2. All groups demonstrated positivity to Runx2 protein (Figure 4) on the 2nd week post-surgery. In this period, the highest quantity of this protein was detected on group IV (sham) and was present in the whole defect. The occupancy rates of Runx2 in the autograft (group I) and PRP associated with autograft (group II) were similar and occupied the area that surrounded the bone graft; in contrast, in group III, the positivity to Runx2 occurred in the scarce cells among the mesenchymal tissue. Furthermore, in all groups, the percentage to Runx2 decreased significantly on the 4th and 6th (Figure 5) post-surgery week as soon as bone matrix, fibrosis, or adipose tissues were formed.

CD34. CD34 cells were present in all groups at 2 weeks post-surgery (Figure 6A). The L-PRP-treated groups demonstrated the highest percentage of $CD34^+$ cells, which occupied the entire area between the grafted bone fragment in group II and forming spindle cells in fibrous tissue on group III. The L-PRP-free groups presented a lower percentage of CD34 cells. They were concentrated in the mature medullary area and/or expressed in the endothelial cells. On the 4th and 6th post-operative weeks, the immunopositivity of the CD34 showed a similar pattern in all groups, although the ratio of the positive cells decreased while the fibrosis or fat cells appeared.

CD45. CD45-positive cells were identified, especially in groups I, II, and IV (Figure 6B). In the L-PRP-free groups, they were seen only in the medullary tissue and in cells that exhibited lymphoid and myeloid morphology in all periods analyzed. In contrast, in the group with L-PRP associated with autograft, a substantial number of immunostained cells were present, occupying the entire area surrounding the grafted bone fragment on the 2nd post-operative week. The percentage of $CD45^+$ cells decreased significantly on the 4th and 6th post-surgery weeks as soon as the bone matrix or adipose tissues were found.

DISCUSSION

The premise regarding the use of PRP in bone repair is based on the significant number of platelets that synthesizes a variety of active growth factors in response to

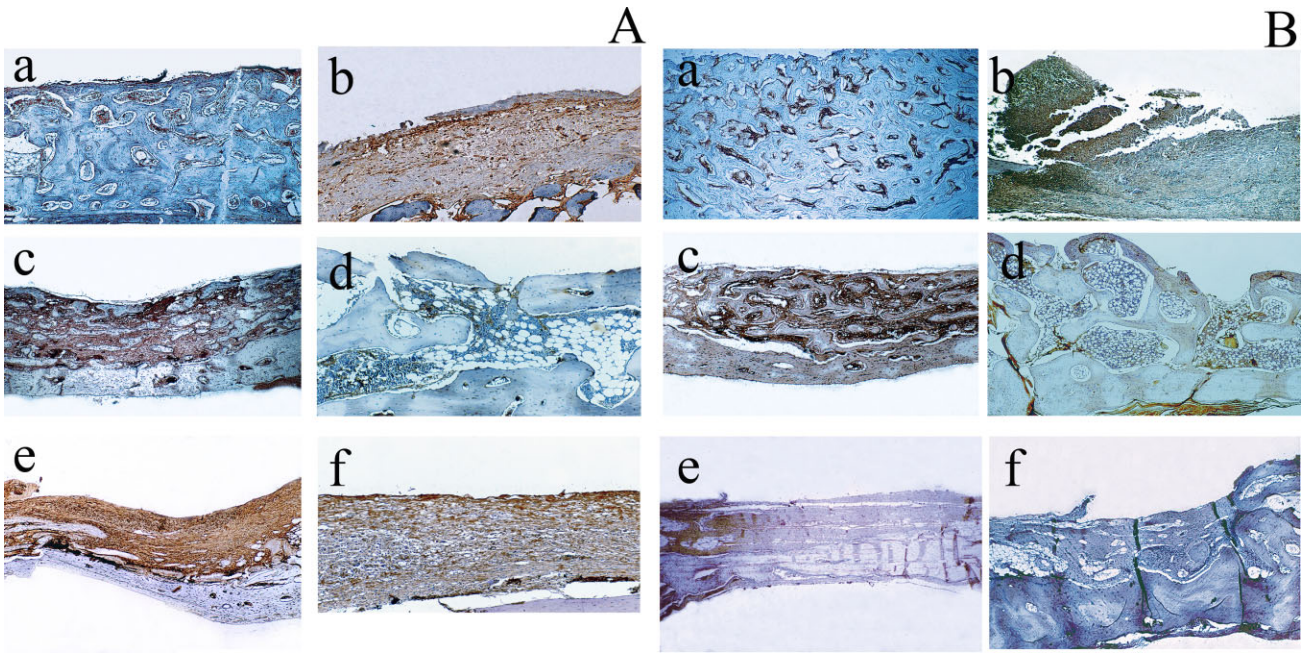

Figure 6 Micrograph A give the immunohistochemical features of the CD34 in the specimens. Micrograph a and b demonstrate the immunopositiviy to autograft and sham group on 2nd week post-surgery. The c and d micrograph reveal the immunopositivity of the CD34 in the autograft mixed o PRP group on 2nd and 6th week post-surgery, respectively, while e and f reveal the CD34+ cells in the group treated with only PRP on the 2nd and 6th week post-surgery. The micrograph B shows the immunohistochemical features of the CD45. Micrographs a and b show the immunopositiviy to CD45 in autograft and sham group on 2nd week post-surgery. The micrograph c and d reveal the immunostain of the CD34 in the autograft mixed to PRP group on the 2nd and 6th week post-surgery, while E and F reveal the CD45+ cells in the group treated with only PRP on 2nd and 6th week post-surgery (magnification ×40, except Aa and Ba, ×100).

indirect collagen interactions at the injured site, regardless of whether it is natural or artificial.[4,5,36] These growth factors can have a major impact on chemotaxy, proliferation, regulation, and differentiation of mesenchymal cells.[3,8,37,38]

Despite the fact that activation of these growth factors by platelets also contribute to osteoneogenesis, results demonstrating that PRP may increase local bone formation[13,39] is in controversy and have not been confirmed by other groups.[40,41] The lack of agreement about the positive effect of PRP on osteoneogenesis is related to the fact that PRP usually is combined with potentially osteoconductive biomaterials, as, for example, autograft, obscuring any real effect of PRP.[42] Also, variations in the PRP preparations that could alter the platelet quality and/or quantity would result in differences in the regenerative potential of PRP.[11]

In fact, the method of PRP preparation, the activation of PRP, as well as the amount of the PRP inserted in the bone defect seem to be important factors that strongly influence the results of the bone repair and help to explain differences in the results in osteogenesis induced by PRP.

An issue that should be taken into consideration in the variation in the PRP preparation is the possible presence or variation of the amount of leukocytes.[12] There is evidence in the literature to suggest that these white blood cells in PRP may be beneficial in healing. In contrast, there is also evidence to suggest that the presence of leukocytes in PRP will lead to increased inflammation and localized fibrosis.[43] The possible negative effect triggered by leukocytes comes from the hypothesis that these white cells liberate proteases that could either reduce the concentrations of growth factors, as occurs in the usual granulation tissue, or increase the potential of growth factors, producing an unfavorable response of fibrosis, similarly to fibrotic disorders.[44,45]

Based on these hypotheses, herein, we studied the microscopic effect of L-PRP alone and mixed to bone autograft in a similar proportion that is considered as an optimal ratio established in the study performed by Nagata and colleagues.[46,47] To minimize the variation of our results, the activation of the L-PRP was performed similarly to other papers described in the literature, that is, using 0.05 ml of 10% calcium chloride/ml of PRP.[46,47]

Nevertheless, the microscopic results presented in this study did not reveal beneficial effects of L-PRP (alone and associated with autograft) on bone formation. Rabbits treated with L-PRP revealed reduced bone matrix deposition and enlarged medullary areas. These findings coincided especially with expressive immunopositivity of TGF-β1 both in cells and extracellular matrix that occupied the entire defect. These results did not corroborate the findings reported by Marx,[13] who demonstrated the expression of TGF-β1 only in bone matrix and surrounding the blood vessel.

Thus, our results indicated that the intense expression of TGF-β1 in the groups with L-PRP might have contributed to the impairment of the usual craniofacial bone repair.

To recognize the effect of the bone repair that occurred in the L-PRP group, it is necessary to interpret the results that were found in groups I (autograft) and IV (sham). In these groups, we observed the presence of CD34 and CD45 isolated in all time periods. The $CD34^+$ cells were primarily concentrated in the endothelium that surrounded vascular tissue and/or spread across the medullary area. The $CD45^+$ cells were identified in specific *loci* that coincided with apparent mature myeloid and lymphoid cell lineage (Figure 4), suggesting a rapid cellular maturation.[24,25]

At the same time, groups I and IV also demonstrated a robust bone matrix deposition. These results were consistent with the elevated percentage of BMP2 protein, concomitant to significant BMPR1B and Runx2 expressions, while the expression of the TGF-β1 was scarce at all time periods analyzed. Thus, these findings together support the hypothesis that bone repair might have occurred through the BMP2 signaling, where the association between this morphogenetic protein and its receptor IB may propagate signals and induce osteoblastic maturation via Runx2. The consequence of these pathways is osteoblastic differentiation and the presence of matrix minerals deposited similarly to typical calvarias bone repair.[48–51]

In contrast, the groups filled with L-PRP demonstrated a lower bone matrix deposited and enlargement of the medullary area, which also mimicked a pathological phenotype. Peculiarly, the medullary area formed on the L-PRP groups demonstrated different histophenotypes and also showed different proteins to calvaria bone repair treated with only L-PRP when compared to L-PRP mixed with autograft.

We identified on the rabbit calvaria treated only with L-PRP (group III) prevalence to TGF-β1 expression among cells that presented spindle morphology on the 2nd post-surgery week. In addition, the majority cells of were shown to be $CD34^+CD45^-$ phenotype, and they were interpreted as multipotent stem cells. These results together suggest that the L-PRP alone does not induce an osteoconductor effect because it occurred in the absence of significant presence of BMP2, but also promoted the chemotaxis of multipotent hematopoietic stem cell lineage in the earliest period of repair.[20,52,53] So, in thesis, these $CD34^+CD45^-$ may have the capacity to differentiate into any tissue, but in this study, these cells failed in the bone development associated with lack of the immunopositivity to BMP2. Thus, the reparative frame produced herein coincided with fibrosis, presented on the 4th and 6th post-surgery weeks, on the marked presence of the TGF-β1 protein in all time periods.

The fibrotic frame induced by L-PRP was consistent with the findings of previous studies.[54,55] Two different hypotheses should be taken into consideration when attempting to explain the results of this study. The first hypothesis involves possible platelet–collagen interactions mimicking a thrombogenic-like effect, given that the activated platelets contain specific sites for different types of collagen interaction in its cellular membrane[56–60] and also express TGF-β1. This hypothesis was suggested recently by our group,[14] who noted a similar ratio between collagens I and III on the defect treated with PRP in rabbit calvarias. Thus, the excess of collagen III was highlighted as the fundamental issue that contributed to a decrease of the bone matrix deposited when PRP was used, given that collagen III is found only at the endosteal surface of bone but never within the bone matrix or surrounding or supporting the adhesion of bone cells.[61]

A second hypothesis that may help to explain the fibrotic process when PRP is used involves the persistent presence of TGF-β1 at the injury sites, given that this growth factor is also a fibrogenic cytokine.[62–64] Based on this hypothesis, Giovanini and colleagues[65] studied the craniofacial bone repair associated with PRP and found a close relationship among the higher quantities of the TGF-β (≈18× higher in the PRP group), the largest presence of collagen III, and the greater number of myofibroblasts present in all time periods analyzed. The authors indicated that these three factors acting together

would produce a feedforward event that led to a mechanism coordinated by TGF-β which might promote and maintain myofibroblast differentiation during the same time that pathological fibrosis were built.

On other hand, in the defects treated with L-PRP mixed with autograft (group II), we identified scarce expression of the BMP2 concentrated to bone fragment engrafted adjacencies, and a higher quantity of the cells that expressed positivity to concomitant BMPR1B, Runx2, and TGF-β1 especially in the earlier stages of the repair. Moreover, at the same time, these cells also exhibited $CD34^{+}CD45^{+/-}$ immunophenotype.

Intriguingly, the simultaneous presence of the $BMPR1B^{+}$ $Runx2^{+}$ and $CD34^{+}CD45^{+/-}$ proteins is an uncommon finding because BMPR1B and Runx2 expressions are not present in either hematopoietic stem cells or differentiated hematopoietic cells.[66] Also, these clusters of differentiation expressed simultaneously are restricted to hematopoietic stem cell lineage.

The interpretation of these results suggest that, in fact, L-PRP may increase the number of osteoprogenitor cells ($BMPR1B^{+}$ and $Runx2^{+}$ lineage) when associated with bone fragments as a scaffold and in the presence of the TGF-β1 in the early period of repair. However, the L-PRP also hindered the final stages of bone development, as evidenced herein by the failure in the bone matrix deposited even in the presence of Runx2.

A likely explanation for these results could be an antagonism expression between TGF-β1 and BMP2 on the critical stage of the repair (2nd week). Consistent with this hypothesis, Spinella-Jaegle and colleagues[67] reported that TGF-β1 and BMP2 did not seem to have the same biological activities in cells of the osteoblastic lineage. Furthermore, they found that their effects on osteoblastic cell differentiation and maturation differed substantially. In contrast, BMP2 induced the differentiation of stem cells toward the osteoblastic lineage; TGF-β opposed the effect of BMPs on osteoblastic cell maturation, thus hindering the terminal osteoblast differentiation.

It is important to highlight the fact that BMP2 as well as TGF-β1 even induces Runx2 expression via BMPR1B. Nevertheless, the findings published by Kang and colleagues[68] demonstrated that, differently from BMP2, the TGF-β1 suppresses the protein osteogenic function of Runx2, preventing the production of alkaline phosphatase and impairing the production of bone tissue.

Thus, these hypotheses together may be built in our study, since we found intense $TGF\text{-}\beta1^{+}$, concomitant to $BMPR1B^{+}$ and $Runx2^{+}$, and lack of BMP2 simultaneously to the absence of robust bone matrix deposition.

Moreover, another important result in this study involved the simultaneous expression between $TGF\beta1^{+}$ $BMPR1B^{+}$ $Runx2^{+}$ and both $CD34^{+}CD45^{+/-}$ lineages, especially on the 2nd week post-surgery, associated with adipose tissue development in the defect treated with L-PRP associated with autograft on the 4th and 6th weeks post-surgery. Based on these results (immunohistochemical and histological), we suggested that the fat cell development might have occurred by cellular transdifferentiation from osteolineage cells (Runx2+) through hematopoietic stem cell interconversion ($CD34^{+}CD45^{+/-}$),[15,16,69] producing a bone phenotype similarly to osteoporosis (Figure 1). This hypothesis is supported by the findings published by Chen and colleagues[34] and Wan and colleagues,[31] who demonstrated *in vitro* that overexpression signaling through BMPR1B associated with the absence of BMP2 in osteoblastic lineage not only dramatically impaired the osteoneogenesis but also contributed to adipocytes differentiation, a fact that may be also correlated with the decrease of TGF-β1, which is a natural adipose inhibitor.[70]

However, it is necessary to point out that this study has some limitations. First, the initial analysis was completed after only 2 weeks; therefore, no conclusions regarding the immediate effects of L-PRP can be drawn. Second, immunohistochemistry staining only identifies the presence or absence of proteins, regardless of the time at which they were expressed and the effectiveness of the differentiation process.[71] Third, the bone repair associated with BMP2 and BMPR1B is a usual pathway to craniofacial repair and our results could not be applied to appendicular or axial bone repair, given that they express different proteins and are derived from distinct embryological sources.[72,73] Nevertheless, the present data may contribute to the discussion about the clinical use of L-PRP.

CONCLUSION

Based on the results of this study, it can be concluded that the use of L-PRP enriched 5× may hinder bone matrix development since the BMP2 expression in the specimens treated with L-PRP was scarce. In addition, the use of L-PRP also induced a medullary pathological phenotype distinct when used alone or mixed with

autograft. When used alone, the L-PRP induced fibrosis connected with intense positivity to TGF-β1 in all time periods analyzed. On other hand, when L-PRP was mixed to autograft, it induced the presence of the osteolineage cells (BMPR1B+ Runx2+), but also inhibited the terminal osteoblastic maturation associated with the lack of BMP2 and the presence of TGF-β 1+, facts that contributed to cellular transdifferentiation into fat cells.

ACKNOWLEDGMENTS

This work was supported by the Histopathology Laboratory of Positivo University. The authors would like to thank Mr. Paulo Henrique de Jesus for the skilled technical assistance.

REFERENCES

1. Aghaloo TL, Moy PK, Freymiller EG. Evaluation of platelet-rich plasma in combination with anorganic bovine bone in the rabbit cranium: a pilot study. Int J Oral Maxillofac Implants 2004; 19:59–65.
2. Freymiller EG, Aghaloo TL. Platelet-rich plasma: ready or not? J Oral Maxillofac Surg 2004; 62:484–488.
3. Marx RE. Platelet-rich plasma: evidence to support its use. J Oral Maxillofac Surg 2004; 62:489–496.
4. Nieswandt B, Watson SP. Platelet-collagen interaction: is GPVI the central receptor? Blood 2003; 102:449–461.
5. Roberts DE, McNicol A, Bose R. Mechanism of collagen activation in human platelets. J Biol Chem 2004; 279:19421–19430.
6. Eppley BL, Woodell JE, Higgins J. Platelet quantification and growth factor analysis from platelet-rich plasma: implications for wound healing. Plast Reconstr Surg 2004; 114:1502–1508.
7. Mooren RE, Hendriks EJ, van den Beucken JJ, et al. The effect of platelet-rich plasma in vitro on primary cells: rat osteoblast-like cells and human endothelial cells. Tissue Eng Part A 2010; 16:3159–3172.
8. Intini G. The use of platelet-rich plasma in bone reconstruction therapy. Biomaterials 2009; 30:4956–4966.
9. Nikolidakis D, Jansen JA. The biology of platelet-rich plasma and its application in oral surgery: literature review. Tissue Eng Part B Rev 2008; 14:249–258.
10. Balaguer T, Boukhechba F, Clave A, et al. Biphasic calcium phosphate microparticles for bone formation: benefits of combination with blood clot. Tissue Eng Part A 2010; 16:3495–3505.
11. Arnoczky SP, Delos D, Rodeo SA. What is platelet-rich plasma? Operative techniques in sports. Medicine 2011; 19:142–148.
12. Dohan Ehrenfest DM, Rasmusson L, Albrektsson T. Classification of platelet concentrates: from pure platelet-rich plasma (P-PRP) to leucocyte- and platelet-rich fibrin (L-PRF). Trends Biotechnol 2009; 27:158–167.
13. Marx RE, Carlson ER, Eichstaedt RM, Schimmele SR, Strauss JE, Georgeff KR. Platelet-rich plasma: growth factor enhancement for bone grafts. Oral Surg Oral Med Oral Pathol Oral Radiol Endod 1998; 85:638–646.
14. Giovanini AF, Deliberador TM, Gonzaga CC, et al. Platelet-rich plasma diminishes calvarial bone repair associated with alterations in collagen matrix composition and elevated CD34+ cell prevalence. Bone 2010; 46:1597–1603.
15. Gimble JM, Zvonic S, Floyd ZE, Kassem M, Nuttall ME. Playing with bone and fat. J Cell Biochem 2006; 98:251–266.
16. Kassem M, Abdallah BM, Saeed H. Osteoblastic cells: differentiation and trans-differentiation. Arch Biochem Biophys 2008; 473:183–187.
17. Schaffler A, Muller-Ladner U, Scholmerich J, Buchler C. Role of adipose tissue as an inflammatory organ in human diseases. Endocr Rev 2006; 27:449–467.
18. Zhou L, Nguyen AN, Sohal D, et al. Inhibition of the TGF-beta receptor I kinase promotes hematopoiesis in MDS. Blood 2008; 112:3434–3443.
19. Fortunel NO, Hatzfeld A, Hatzfeld JA. Transforming growth factor-beta: pleiotropic role in the regulation of hematopoiesis. Blood 2000; 96:2022–2036.
20. Majeti R, Park CY, Weissman IL. Identification of a hierarchy of multipotent hematopoietic progenitors in human cord blood. Cell 2007; 1:635–645.
21. Chen CZ, Li L, Lodish HF, Bartel DP. MicroRNAs modulate hematopoietic lineage differentiation. Science 2004; 303: 83–86.
22. Paquette R, Dorshkind K. Optimizing hematopoietic recovery following bone marrow transplantation. J Clin Invest 2002; 109:1527–1528.
23. Shivtiel S, Kollet O, Lapid K, et al. CD45 regulates retention, motility, and numbers of hematopoietic progenitors, and affects osteoclast remodeling of metaphyseal trabecules. J Exp Med 2008; 205:2381–2395.
24. Craig W, Poppema S, Little MT, Dragowska W, Lansdorp PM. CD45 isoform expression on human haemopoietic cells at different stages of development. Br J Haematol 1994; 88:24–30.
25. Penninger JM, Irie-Sasaki J, Sasaki T, Oliveira-dos-Santos AJ. CD45: new jobs for an old acquaintance. Nat Immunol 2001; 2:389–396.
26. Oki Y, Watanabe S, Endo T, Kano K. Mature adipocyte-derived dedifferentiated fat cells can trans-differentiate into osteoblasts in vitro and in vivo only by all-trans retinoic acid. Cell Struct Funct 2008; 33:211–222.
27. Rosen V. BMP2 signaling in bone development and repair. Cytokine Growth Factor Rev 2009; 20:475–480.
28. Wang Q, Huang C, Xue M, Zhang X. Expression of endogenous BMP-2 in periosteal progenitor cells is essential for bone healing. Bone 2011; 48:524–532.

29. Abzhanov A, Rodda SJ, McMahon AP, Tabin CJ. Regulation of skeletogenic differentiation in cranial dermal bone. Development 2007; 134:3133–3144.
30. Nie X, Luukko K, Kettunen P. BMP signalling in craniofacial development. Int J Dev Biol 2006; 50:511–521.
31. Wan DC, Shi YY, Nacamuli RP, Quarto N, Lyons KM, Longaker MT. Osteogenic differentiation of mouse adipose-derived adult stromal cells requires retinoic acid and bone morphogenetic protein receptor type IB signaling. Proc Natl Acad Sci U S A 2006; 103:12335–12340.
32. Sahni V, Mukhopadhyay A, Tysseling V, et al. BMPR1a and BMPR1b signaling exert opposing effects on gliosis after spinal cord injury. J Neurosci 2010; 30:1839–1855.
33. Ashique AM, Fu K, Richman JM. Signalling via type IA and type IB bone morphogenetic protein receptors (BMPR) regulates intramembranous bone formation, chondrogenesis and feather formation in the chicken embryo. Int J Dev Biol 2002; 46:243–253.
34. Chen D, Ji X, Harris MA, et al. Differential roles for bone morphogenetic protein (BMP) receptor type IB and IA in differentiation and specification of mesenchymal precursor cells to osteoblast and adipocyte lineages. J Cell Biol 1998; 142:295–305.
35. Di Cataldo S, Ficarra E, Acquaviva A, Macii E. Automated segmentation of tissue images for computerized IHC analysis. Comput Methods Programs Biomed 2010; 100:1–15.
36. Boilard E, Nigrovic PA, Larabee K, et al. Platelets amplify inflammation in arthritis via collagen-dependent microparticle production. Science 2010; 327:580–583.
37. Klongnoi B, Rupprecht S, Kessler P, Thorwarth M, Wiltfang J, Schlegel KA. Influence of platelet-rich plasma on a bioglass and autogenous bone in sinus augmentation. An explorative study. Clin Oral Implants Res 2006; 17:312–320.
38. Klongnoi B, Rupprecht S, Kessler P, et al. Lack of beneficial effects of platelet-rich plasma on sinus augmentation using a fluorohydroxyapatite or autogenous bone: an explorative study. J Clin Periodontol 2006; 33:500–509.
39. Fennis JP, Stoelinga PJ, Jansen JA. Mandibular reconstruction: a histological and histomorphometric study on the use of autogenous scaffolds, particulate cortico-cancellous bone grafts and platelet rich plasma in goats. Int J Oral Maxillofac Surg 2004; 33:48–55.
40. Aghaloo TL, Moy PK, Freymiller EG. Investigation of platelet-rich plasma in rabbit cranial defects: a pilot study. J Oral Maxillofac Surg 2002; 60:1176–1181.
41. Jakse N, Tangl S, Gilli R, et al. Influence of PRP on autogenous sinus grafts. An experimental study on sheep. Clin Oral Implants Res 2003; 14:578–583.
42. Pryor ME, Yang J, Polimeni G, et al. Analysis of rat calvaria defects implanted with a platelet-rich plasma preparation: radiographic observations. J Periodontol 2005; 76:1287–1292.
43. Chizzolini C, Brembilla NC, Montanari E, Truchetet ME. Fibrosis and immune dysregulation in systemic sclerosis. Autoimmun Rev 2011; 10:276–281.
44. Sangaletti S, Tripodo C, Cappetti B, et al. SPARC oppositely regulates inflammation and fibrosis in bleomycin-induced lung damage. Am J Pathol 2011; 179:3000–3010.
45. Tomasek JJ, McRae J, Owens GK, Haaksma CJ. Regulation of alpha-smooth muscle actin expression in granulation tissue myofibroblasts is dependent on the intronic CArG element and the transforming growth factor-beta1 control element. Am J Pathol 2005; 166:1343–1351.
46. Nagata MJ, Messora M, Pola N, et al. Influence of the ratio of particulate autogenous bone graft/platelet-rich plasma on bone healing in critical-size defects: a histologic and histometric study in rat calvaria. J Orthop Res 2010; 28:468–473.
47. Nagata M, Messora M, Okamoto R, et al. Influence of the proportion of particulate autogenous bone graft/platelet-rich plasma on bone healing in critical-size defects: an immunohistochemical analysis in rat calvaria. Bone 2009; 45:339–345.
48. Merrill AE, Eames BF, Weston SJ, Heath T, Schneider RA. Mesenchyme-dependent BMP signaling directs the timing of mandibular osteogenesis. Development 2008; 135:1223–1234.
49. Canalis E, Economides AN, Gazzerro E. Bone morphogenetic proteins, their antagonists, and the skeleton. Endocr Rev 2003; 24:218–235.
50. Rawadi G, Vayssiere B, Dunn F, Baron R, Roman-Roman S. BMP-2 controls alkaline phosphatase expression and osteoblast mineralization by a Wnt autocrine loop. J Bone Miner Res 2003; 18:1842–1853.
51. Roman-Roman S, Garcia T, Jackson A, et al. Identification of genes regulated during osteoblastic differentiation by genome-wide expression analysis of mouse calvaria primary osteoblasts in vitro. Bone 2003; 32:474–482.
52. Fritsch G, Buchinger P, Printz D, et al. Rapid discrimination of early CD34+ myeloid progenitors using CD45-RA analysis. Blood 1993; 81:2301–2309.
53. Strobl H, Takimoto M, Majdic O, et al. Myeloperoxidase expression in CD34+ normal human hematopoietic cells. Blood 1993; 82:2069–2078.
54. Oliveira Filho MA, Nassif PA, Malafaia O, et al. Effects of a highly concentrated platelet-rich plasma on the bone repair using non-critical defects in the calvaria of rabbits. Acta Cir Bras 2010; 25:28–33.
55. Choi BH, Im CJ, Huh JY, Suh JJ, Lee SH. Effect of platelet-rich plasma on bone regeneration in autogenous bone graft. Int J Oral Maxillofac Surg 2004; 33:56–59.
56. Fauvel F, Legrand YJ. Inhibition of type III collagen induced platelet aggregation by active alpha 1 (III) CB4 peptide fragments. Thromb Res 1980; 17:285–287.
57. Chiang TM, Seyer JM, Kang AH. Collagen-platelet interaction: separate receptor sites for types I and III collagen. Thromb Res 1993; 71:443–456.

58. Chiang TM, Zhu J, Woo-Rasberry V. Peptides derived from platelet non-integrin collagen-receptors or types I and III collagen inhibit collagen-platelet interaction. Cardiovasc Hematol Disord Drug Targets 2007; 7:71–75.
59. Sakariassen KS, Joss R, Muggli R, et al. Collagen type III induced ex vivo thrombogenesis in humans. Role of platelets and leukocytes in deposition of fibrin. Arteriosclerosis 1990; 10:276–284.
60. Zhu J, Cole F, Woo-Rasberry V, Fang XR, Chiang TM. Type I and type III collagen-platelet interaction: inhibition by type specific receptor peptides. Thromb Res 2007; 119:111–119.
61. Gronthos S, Stewart K, Graves SE, Hay S, Simmons PJ. Integrin expression and function on human osteoblast-like cells. J Bone Miner Res 1997; 12:1189–1197.
62. Wynn TA. Common and unique mechanisms regulate fibrosis in various fibroproliferative diseases. J Clin Invest 2007; 117:524–529.
63. Wells RG. Fibrogenesis. V. TGF-beta signaling pathways. Am J Physiol Gastrointest Liver Physiol 2000; 279:G845–G850.
64. Pohlers D, Brenmoehl J, Loffler I, et al. TGF-beta and fibrosis in different organs – molecular pathway imprints. Biochim Biophys Acta 2009; 1792:746–756.
65. Giovanini AF, Gonzaga CC, Zielak JC, et al. Platelet-rich plasma (PRP) impairs the craniofacial bone repair associated with its elevated TGF-beta levels and modulates the co-expression between collagen III and alpha-smooth muscle actin. J Orthop Res 2011; 29:457–463.
66. Zhang J, Niu C, Ye L, et al. Identification of the haematopoietic stem cell niche and control of the niche size. Nature 2003; 425:836–841.
67. Spinella-Jaegle S, Roman-Roman S, Faucheu C, et al. Opposite effects of bone morphogenetic protein-2 and transforming growth factor-beta1 on osteoblast differentiation. Bone 2001; 29:323–330.
68. Kang JS, Alliston T, Delston R, Derynck R. Repression of Runx2 function by TGF-beta through recruitment of class II histone deacetylases by Smad3. EMBO J 2005; 24:2543–2555.
69. Gimble JM, Nuttall ME. Bone and fat: old questions, new insights. Endocrine 2004; 23:183–188.
70. Choy L, Derynck R. Transforming growth factor-beta inhibits adipocyte differentiation by Smad3 interacting with CCAAT/enhancer-binding protein (C/EBP) and repressing C/EBP transactivation function. J Biol Chem 2003; 278:9609–9619.
71. Thorwarth M, Wehrhan F, Schultze-Mosgau S, Wiltfang J, Schlegel KA. PRP modulates expression of bone matrix proteins in vivo without long-term effects on bone formation. Bone 2006; 38:30–40.
72. Akintoye SO, Lam T, Shi S, Brahim J, Collins MT, Robey PG. Skeletal site-specific characterization of orofacial and iliac crest human bone marrow stromal cells in same individuals. Bone 2006; 38:758–768.
73. van den Bos T, Speijer D, Bank RA, Bromme D, Everts V. Differences in matrix composition between calvaria and long bone in mice suggest differences in biomechanical properties and resorption: special emphasis on collagen. Bone 2008; 43:459–468.